Contents

1 Introduction

The experiment is about the iodine spectroscopy. We will have a closer look at the $X^1\Sigma^+_{0g} \leftrightarrow B^3\Pi^+_{0u}$ transition. With this experiment we first start with measuring the absorption spectrum of iodine and want to determine the oscillation constants $\omega'_e x_e$ and ω_e with help of the Birge-Sponer plot. We will also measure the dissociation energy D_e with the Morse potential and with the term differences. In addition to that we will determine the excitation energy T'_e and the energy E_{diss} where the electron dissociates. Finally we plot the Morse potential with the obtained data.
The second part is about the emission of iodine. We measure transitions which are excited by a helium-neon laser and identify them. After that we want to determine Franck-Condon factors and we will compare the expected intensity with the measured ones.

2 Physical background

2.1 Born-Oppenheimer approximation

In this experiment we examine a diatomic molecule. In this case it is helpful to use an approximation for calculating the solutions of the Schrödinger equations because of their complexity. One example is given by the Born-Oppenheimer approximation.
The approximation says that it is possible to separate the movement of the electrons and the nuclei in two different wave functions

$$\Psi(r_{i,R_j}) = \Psi_{vib} \cdot \Psi^{\,0}_{k}(r_i, R_j), \tag{1}$$

where Ψ_{vib} : nuclei wave function and
$\Psi^{\,0}_{k}(r_i, R_j)$: electron wave function.

This hypothesis is justified because of the different masses of electrons and nuclei. Nuclei are much heavier than electrons. The consequence is that the movement of nuclei are much slower than of the electrons and so the electrons have the ability to adapt oneself nearly instantaneous to a new nucleus position.

2.2 Electronic transitions

An electronic transition can be stimulated by radiation. The radiation transfer its energy to an electron of the atom. Therefore it has a higher energy level. On the other hand it is also possible that the stimulated electron goes back to a lower state by emitting radiation. However, not every transition is permitted, there are different selection rules

- $g \leftrightarrow u$, $g \nleftrightarrow g$, $u \nleftrightarrow u$
- $\Delta\Omega = 0, +1, -1$
- $\Delta\Lambda = 0, +1, -1$ (coupling case c)
- $\Delta S = 0$ (coupling case a)

where Ω : projection total angular momentum
Λ: projection orbital angular momentum
S: total electron spin.

Both projections are regarding to the molecule axis. The last two conditions are not generally correct. They are special cases of some Hund's coupling cases. For this experiment there is only one interesting transition which can be detected by our experimental setup:

$$X^1\Sigma_{0g}^+ \leftrightarrow B^3\Pi_{0u}^+. \tag{2}$$

This confirms to coupling case c because of a strong spin orbit coupling. $X^1\Sigma_{0g}^+$ is the basic state of Iodine.

2.3 Franck-Condon principle

An electronic transition is very fast and has nearly no influence on the kinetic energy of the nuclei, so the distance between the nuclei does not change. Because of the constant distance you can visualize the transition with a vertical line in a potential curves diagram (cf. Figure 1).

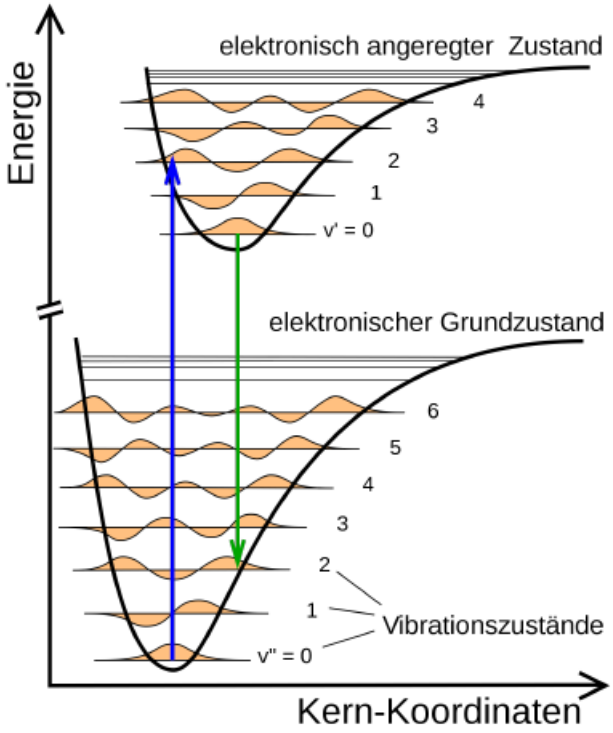

Figure 1: Potential curve diagram for visualizing the Franck-Condon principle [3]

With the Franck-Condon principle ones can say different probabilities for each transition. Decisive for the most possible one is the overlap between the basic and the stimulated state. For describing this phenomena you can use the Franck-Condon factor

$$FC(\nu_\mathrm{i}, \nu_\mathrm{k}) = \left| \int \Psi_\mathrm{vib}(\nu_\mathrm{i}) \Psi_\mathrm{vib}(\nu_\mathrm{k}) dR \right|^2, \tag{3}$$

where Ψ_vib are normalized oscillation wave functions and ν_i, ν_k are oscillation numbers.

2.4 Morse potential

An approximation for calculating the potential energy of a bi-atomic molecule is given by the Morse potential. Ones can describe the potential near the minimum with a parable, but for higher nucleus distances it gets worse. A better formula is the Morse potential

$$E_{\text{pot}}(R) = E_{\text{D}} \cdot \left[1 - e^{-a(R-R_{\text{e}})}\right]^2. \tag{4}$$

Here is R the distance from the atomic nucleus, R_{e} the equilibrium distance, E_{D} the dissociation energy and a is a constant, which can be calculated with

$$a = \sqrt{\frac{4\pi c\mu \cdot \omega_{\text{e}} x_{\text{e}}}{\hbar}} \quad [5](\text{page 11}), \tag{5}$$

while $\mu = 1{,}053 \cdot 10^{-25}\,\text{kg}$[5] (page 11) is the reduced mass of iodine. $\omega_{\text{e}} x_{\text{e}}$ will be explained below. The graph course is shown in Figure 2.

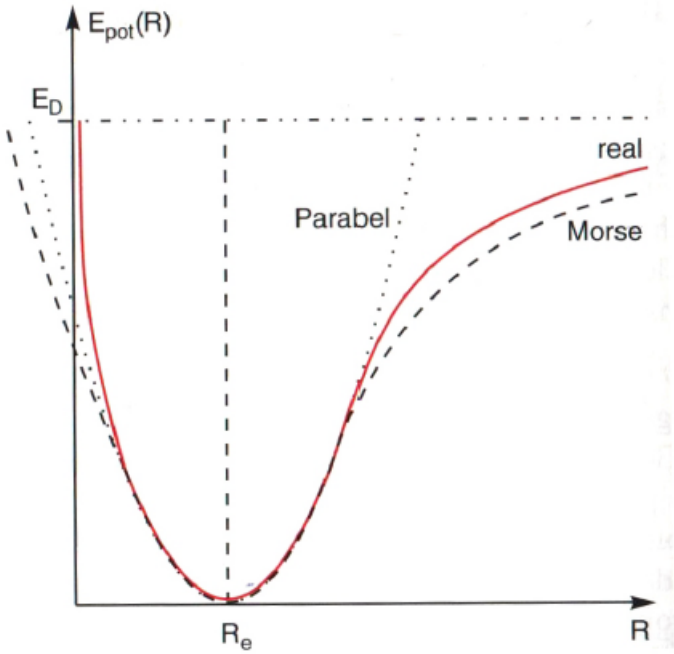

Figure 2: Morse-Potential compared with a parable and the real potential course [3]

As ones can see the Morse potential is quit good for the area around the minimum and for high nuclei distances. For small distances $R \ll R_{\text{e}}$ it gets inaccurate.
The Morse potential is helpful because it contains exactly analytically solutions of the energy eigenstates Ψ_{vib} and energy eigenvalues E_{vib}.

$$E_{\text{vib}}(\nu) = \hbar\omega_{\text{e}}(\nu + \frac{1}{2}) - \hbar\omega_{\text{e}} x_{\text{e}}(\nu + \frac{1}{2})^2 \tag{6}$$

2.5 Birge-Sponer plot

With help of perturbation theory you obtain for the oscillation energies the following series

$$G(\nu) = \omega_{\text{e}}\left(\nu + \frac{1}{2}\right) - \omega_{\text{e}} x_{\text{e}}\left(\nu + \frac{1}{2}\right)^2 + \omega_{\text{e}} y_{\text{e}}\left(\nu + \frac{1}{2}\right)^3 + \ldots \tag{7}$$

With oscillation constants $\omega_{\text{e}} \gg \omega_{\text{e}} x_{\text{e}} \gg \omega_{\text{e}} y_{\text{e}}$. The third order is mentioned in the theoretical background, but it is not important for the experiment. For analysing the experiment

we only consider the first two orders.
It holds for the zero-point-energy

$$G(0) = \frac{1}{2}\omega_e - \frac{1}{4}\omega_e x_e + \frac{1}{8}\omega_e y_e. \tag{8}$$

With this information one can calculate the difference between two oscillation energies.

$$\Delta G(\nu + \frac{1}{2}) := G(\nu+1) - G(\nu) = \omega_e - \omega_e x_e(2\nu+2) + \omega_e y_e(3\nu^2 + 6\nu + \frac{13}{4}) + ... \tag{9}$$

Hence there is only a finite number of oscillation terms inside the potential well we obtain for a special ν_{diss} that $\Delta G(\nu + \frac{1}{2})$ is equal to zero. Above $G(\nu_{\text{diss}})$ the molecule is dissociate. Now one can define two physical sizes:

- dissociation energy D_0:

$$D_0 = \sum_{n=0}^{\nu_{\text{diss}}} \Delta G(\nu + \frac{1}{2}) \tag{10}$$

  which is measured from ν_0 to ν_{diss}

- dissociation energy D_e:

$$D_e = G(0) + D_0 \tag{11}$$

  measured from the minimum of the potential well to ν_{diss}.

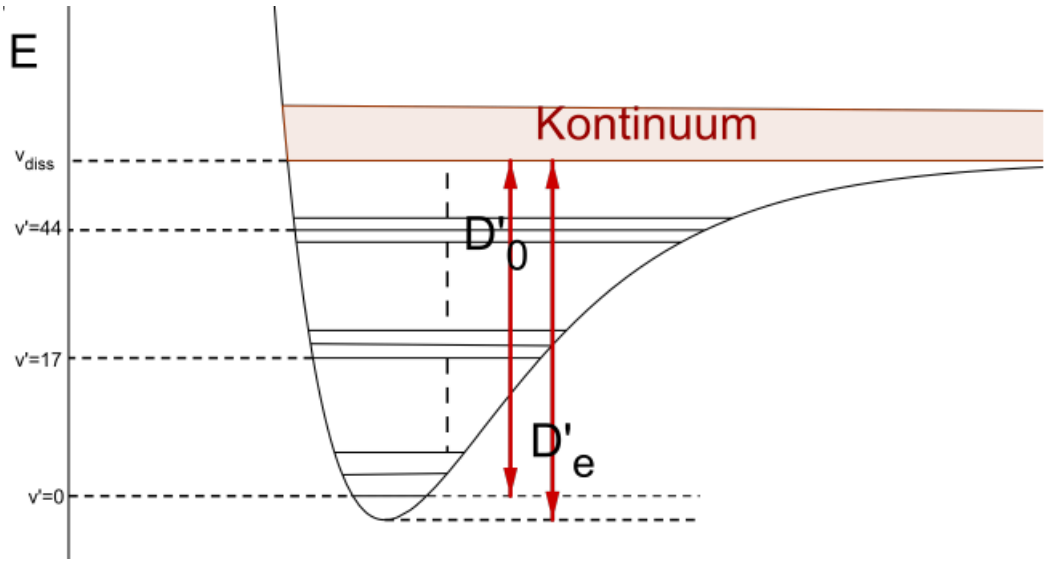

Figure 3: Visualization of D_0 and D_e [3]

For calculating the dissociation energy one can plot $\Delta G(\nu + \frac{1}{2})$ over $\nu + \frac{1}{2}$ and determine the point of intersection of formula 9 and the x-axis.
It is also possible to calculate the dissociation energy D_e in another way. Here we compute the minimum of $G(\nu)$ in formula 7. With setting the derivation equals to zero and and insert the gotten ν again in formula 7 you get

$$D_e = \frac{\omega_e^2}{4\omega_e x_e}. \tag{12}$$

3 Set up

3.1 Absorption

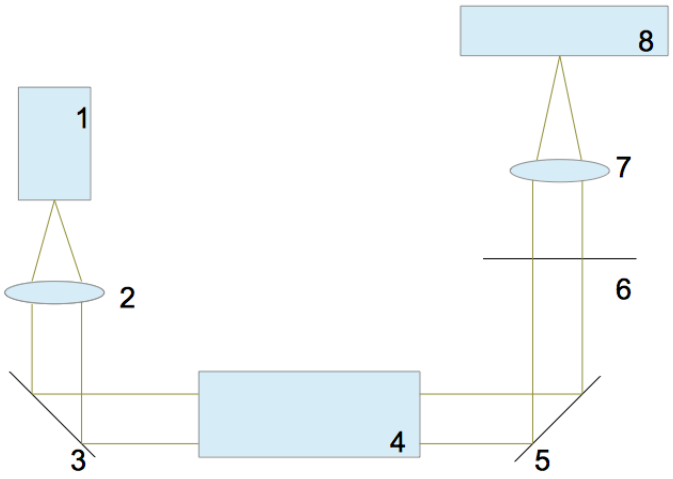

Figure 4: Setup for measuring the absorption [2]

The setup is shown in 4. The light source is a halogen lamp (1) because of its wide light spectrum. To get parallel light there is a lens (2) ($f_1 = 100\,\text{mm}$). Via a mirror (3) the parallel light strokes to the iodine tube (4) and after another mirror (5) to a neutral density filter (6). After the filter there is another lens (7) ($f_2 = 100\,\text{mm}$) for focusing the light to a spectrometer (8). The information of the spectrometer will transmitted to a PC.

3.2 Emission

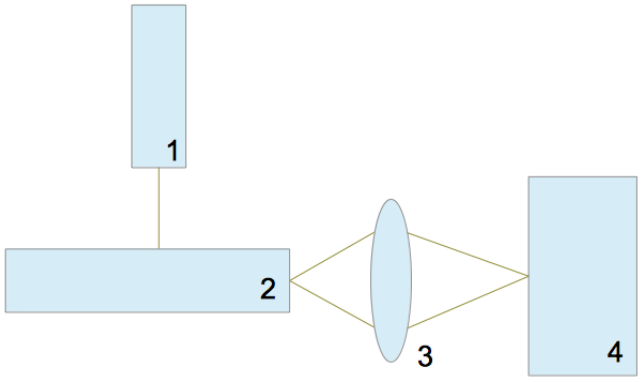

Figure 5: Setup for measuring the emission [2]

The setup for measuring the emission is shown in 5. Now we use a laser (1) which is focused to the iodine (2). So some iodine atoms are in an excited state. These atoms emit photons. These photons are focused with a lens (3) ($f_3 = 70\,\text{mm}$) to a monochromator (4). The information of the monochromator will be amplified by an photomultiplier and then transmitted to a PC.

The spectrometer and the monochromator are explained in the attachment.

4 Execution

4.1 Absorption

Before starting the measurement of absorption it is necessary to set the lenses in the right positions. Therefor we apply a paper in front of the spectrometer and try to focus the filament of the halogen lamp on it. So we get a clear signal later on.
With the program SpectraSuite one can measure the light spectrum after the iodine tube.

4.2 Emission

4.2.1 Calibrate the monochromator

For calibrating the monochromator we use the following setup shown in Figure 6.

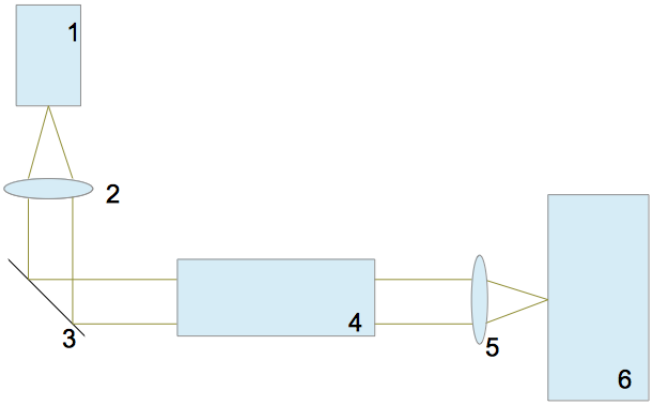

Figure 6: Setup for calibrating the monochromator [2]

It is the setup form the absorption measurement. However we now use a mercury vapor lamp(1) instead of a halogen one and the beam strokes to a lens(5) ($f_2 = 70\,\text{mm}$) which focused the beam to the monochromator. One measure the spectrum from $4000 - 6000$Å. After the calibration measurement we use the proper setup and measure the spectral environmental around the laser light. Therefor we measure from ca. $6100\,\text{Å} - 6500\,\text{Å}$. The second part is to measure the emission spectrum of iodine. Here we use the area from $4000\,\text{Å} - 6000\,\text{Å}$.

5 Analysis

5.1 Absorption spectrum

First step was to acquire the absorption spectrum of iodine between 400 nm and 700 nm. We chosen a scan duration of 3 ms and measured 10.000 times with each more than 10.000 counts per pixel in the relevant area. So we can neglect statistical errors. The program calculated an average which you can see in Figure 7.

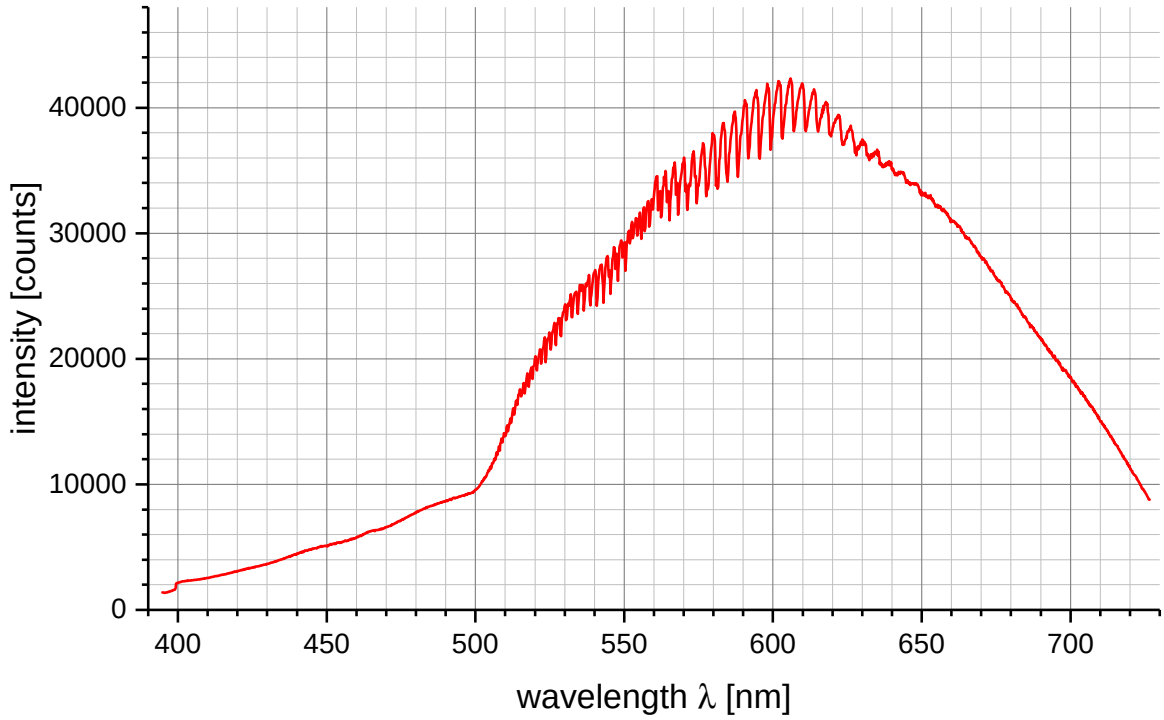

Figure 7: Complete measured absorption spectrum of iodine [1]

From the manual[3] (page 11) we know that the absorption band at $\lambda = 545{,}8\,\text{nm}$ comes from the transition $\nu'' = 0 \rightarrow \nu' = 25$. Beginning with this point we can number the different absorption bands. The transition from $\nu'' = 0 \rightarrow \nu' = 26$ is energy-richer, so it has a smaller wavelength and is consequently on the left side of 25. To take off the wavelengths of each ν'-value with a low uncertainty we decided to make six plots, which have each a range of about 20 nm. On all six plots together are the wavelengths from 500-620 nm and all necessary progressions visible. The graphics are in the appendix (cf. Figures 19-24). Now we read off the wavelengths of all peaks. We decided for a statistical uncertainty of $s_\lambda = 0{,}1\,\text{nm}$, because now the probability for a value out of the one uncertainty area is in our opinion about one-third. There is also a systematic error possible and with a look on $\lambda_{25,\text{theory}} = 545{,}8\,\text{nm}$ and $\lambda_{25,\text{measured}} = (545{,}4 \pm 0{,}1)\,\text{nm}$ even probably, but because we only need the difference of the reciprocal it is in this part negligible. The wavelengths are summed up in Table 1.
To get also the progressions of $\nu'' = 1$ and $\nu'' = 2$, we use that the energy difference between two adjacent ν' values is independent of the underlying progression. So we calculate the difference between two adjacent peaks (within one progression) for all progressions. These are in Table 1. Now we compare the differences between the progressions and look for the best conformity. Here not only the difference conforms but also the ν'. So we have got the ν'''s of all progressions. We suppose that the numbering of the higher two progressions is correct, so there is no uncertainty indicated. The fact that the wavelength differences

between the progressions at $\nu' = 16$ are similar reinforce our supposing.

5.2 Birge-Sponer plot

In a Birge-Sponer diagram we have to plot an energy difference in units of $\frac{1}{\mathrm{m}}$. Therefore we first calculate the reciprocal $k_{\nu'}$ of the wavelength $\lambda_{\nu'}$

$$\begin{aligned} k_{\nu'} &= \frac{1}{\lambda_{\nu'}}, \\ s_{\mathrm{k}_{\nu'}} &= \frac{s_{\lambda_{\nu'}}}{\lambda_{\nu'}^2}, \end{aligned} \tag{13}$$

because it is proportional to the energy. The energy difference can now be computed with

$$\begin{aligned} \Delta G(\nu' + \frac{1}{2}) &= k_{\nu'+1} - k_{\nu'}, \\ s_{\Delta \mathrm{G}} &= \sqrt{s_{\mathrm{k}_{\nu'+1}}^2 + s_{\mathrm{k}_{\nu'}}^2}. \end{aligned} \tag{14}$$

The calculated values are summed up in the tables 2,3 and 4.

	$\nu'' = 0$		$\nu'' = 1$		$\nu'' = 2$	
ν'	$\lambda_{\nu'}$ [nm]	$\lambda_{\nu'} - \lambda_{\nu'+1}$ [nm]	$\lambda_{\nu'}$ [nm]	$\lambda_{\nu'} - \lambda_{\nu'+1}$ [nm]	$\lambda_{\nu'}$ [nm]	$\lambda_{\nu'} - \lambda_{\nu'+1}$ [nm]
6					615,2	4,2
7					611,0	4,0
8					607,0	3,9
9					603,1	3,9
10					599,2	3,6
11					595,6	3,9
12					591,7	3,5
13					588,2	3,4
14			580,9	3,3	584,8	3,3
15			577,6	3,2	581,5	3,3
16	570,6	3,2	574,4	3,2	578,2	3,2
17	567,4	3,0	571,2	3,0	575,0	2,9
18	564,4	3,0	568,2	3,0	572,1	
19	561,4	2,9	565,2	2,7		
20	558,5	2,7	562,5	2,9		
21	555,8	2,9	559,6	2,6		
22	552,9	2,5	557,0	2,6		
23	550,4	2,5	554,4	2,6		
24	547,9	2,5	551,8	2,3		
25	545,4	2,4	549,5	2,4		
26	543,0	2,2	547,1	2,2		
27	540,8	2,2	544,9			
28	538,6	2,2				
29	536,4	2,0				
30	534,4	2,0				
31	532,4	1,9				
32	530,5	1,8				
33	528,7	1,7				
34	527,0	1,8				
35	525,2	1,6				
36	523,6	1,5				
37	522,1	1,3				
38	520,8	1,7				
39	519,1	1,3				
40	517,8	1,2				
41	516,6	1,2				
42	515,4	1,3				
43	514,1	1,1				
44	513,0	1,1				
45	511,9	1,0				
46	510,9	0,9				
47	510,0	1,0				
48	509,0	0,8				
49	508,2	0,9				
50	507,3	0,7				
51	506,6					

Table 1: Distances between the peaks for each progression

ν'	$\nu'+\frac{1}{2}$	$\lambda_{\nu'}$ [nm]	$k_{\nu'}$ $[\frac{1}{\mathrm{mm}}]$	$s_{\mathrm{k}_{\nu'}}$ $[\frac{1}{\mathrm{mm}}]$	$\Delta G(\nu'+\frac{1}{2})$ $[\frac{1}{\mathrm{mm}}]$	$s_{\Delta \mathrm{G}}$ $[\frac{1}{\mathrm{mm}}]$
16	16,5	570,6	1752,5	0,3	9,9	0,4
17	17,5	567,4	1762,4	0,3	9,4	0,4
18	18,5	564,4	1771,8	0,3	9,5	0,4
19	19,5	561,4	1781,3	0,3	9,2	0,5
20	20,5	558,5	1790,5	0,3	8,7	0,5
21	21,5	555,8	1799,2	0,3	9,4	0,5
22	22,5	552,9	1808,6	0,3	8,2	0,5
23	23,5	550,4	1816,9	0,3	8,3	0,5
24	24,5	547,9	1825,2	0,3	8,4	0,5
25	25,5	545,4	1833,5	0,3	8,1	0,5
26	26,5	543,0	1841,6	0,3	7,5	0,5
27	27,5	540,8	1849,1	0,3	7,6	0,5
28	28,5	538,6	1856,7	0,3	7,6	0,5
29	29,5	536,4	1864,3	0,3	7,0	0,5
30	30,5	534,4	1871,3	0,4	7,0	0,5
31	31,5	532,4	1878,3	0,4	6,7	0,5
32	32,5	530,5	1885,0	0,4	6,4	0,5
33	33,5	528,7	1891,4	0,4	6,1	0,5
34	34,5	527,0	1897,5	0,4	6,5	0,5
35	35,5	525,2	1904,0	0,4	5,8	0,5
36	36,5	523,6	1909,9	0,4	5,5	0,5
37	37,5	522,1	1915,3	0,4	4,8	0,5
38	38,5	520,8	1920,1	0,4	6,3	0,5
39	39,5	519,1	1926,4	0,4	4,8	0,5
40	40,5	517,8	1931,2	0,4	4,5	0,5
41	41,5	516,6	1935,7	0,4	4,5	0,5
42	42,5	515,4	1940,2	0,4	4,9	0,5
43	43,5	514,1	1945,1	0,4	4,2	0,5
44	44,5	513,0	1949,3	0,4	4,2	0,5
45	45,5	511,9	1953,5	0,4	3,8	0,5
46	46,5	510,9	1957,3	0,4	3,5	0,5
47	47,5	510,0	1960,8	0,4	3,9	0,5
48	48,5	509,0	1964,6	0,4	3,1	0,5
49	49,5	508,2	1967,7	0,4	3,5	0,5
50	50,5	507,3	1971,2	0,4	2,7	0,6
51	51,5	506,6	1973,9	0,4	-	-

Table 2: wavelengths, energies and energy differences of the progression $\nu'' = 0$

ν'	$\nu'+\frac{1}{2}$	$\lambda_{\nu'}$ [nm]	$k_{\nu'}$ $[\frac{1}{\text{mm}}]$	$s_{\text{k}_{\nu'}}$ $[\frac{1}{\text{mm}}]$	$\Delta G(\nu'+\frac{1}{2})$ $[\frac{1}{\text{mm}}]$	$s_{\Delta\text{G}}$ $[\frac{1}{\text{mm}}]$
14	14,5	580,9	1721,5	0,3	9,8	0,4
15	15,5	577,6	1731,3	0,3	9,6	0,4
16	16,5	574,4	1740,9	0,3	9,8	0,4
17	17,5	571,2	1750,7	0,3	9,2	0,4
18	18,5	568,2	1759,9	0,3	9,3	0,4
19	19,5	565,2	1769,3	0,3	8,5	0,4
20	20,5	562,5	1777,8	0,3	9,2	0,4
21	21,5	559,6	1787,0	0,3	8,3	0,5
22	22,5	557,0	1795,3	0,3	8,4	0,5
23	23,5	554,4	1803,8	0,3	8,5	0,5
24	24,5	551,8	1812,3	0,3	7,6	0,5
25	25,5	549,5	1819,8	0,3	8,0	0,5
26	26,5	547,1	1827,8	0,3	7,4	0,5
27	27,5	544,9	1835,2	0,3	-	-

Table 3: wavelengths, energies and energy differences of the progression $\nu''=1$

ν'	$\nu'+\frac{1}{2}$	$\lambda_{\nu'}$ [nm]	$k_{\nu'}$ $[\frac{1}{\text{mm}}]$	$s_{\text{k}_{\nu'}}$ $[\frac{1}{\text{mm}}]$	$\Delta G(\nu'+\frac{1}{2})$ $[\frac{1}{\text{mm}}]$	$s_{\Delta\text{G}}$ $[\frac{1}{\text{mm}}]$
6	6,5	615,2	1625,5	0,3	11,2	0,4
7	7,5	611,0	1636,7	0,3	10,8	0,4
8	8,5	607,0	1647,4	0,3	10,7	0,4
9	9,5	603,1	1658,1	0,3	10,8	0,4
10	10,5	599,2	1668,9	0,3	10,1	0,4
11	11,5	595,6	1679,0	0,3	11,1	0,4
12	12,5	591,7	1690,0	0,3	10,1	0,4
13	13,5	588,2	1700,1	0,3	9,9	0,4
14	14,5	584,8	1710,0	0,3	9,7	0,4
15	15,5	581,5	1719,7	0,3	9,8	0,4
16	16,5	578,2	1729,5	0,3	9,6	0,4
17	17,5	575,0	1739,1	0,3	8,8	0,4
18	18,5	572,1	1747,9	0,3	-	-

Table 4: wavelengths, energies and energy differences of the progression $\nu''=2$

For the Birge-Sponer plot we plotted $\Delta G(\nu+\frac{1}{2})$ over $\nu+\frac{1}{2}$ like discussed in the theoretical background (see 2.5). We did this for $\nu''=0$, $\nu''=1$ and $\nu''=2$ the graphs are shown in Figure 8, Figure 9 and Figure 10.

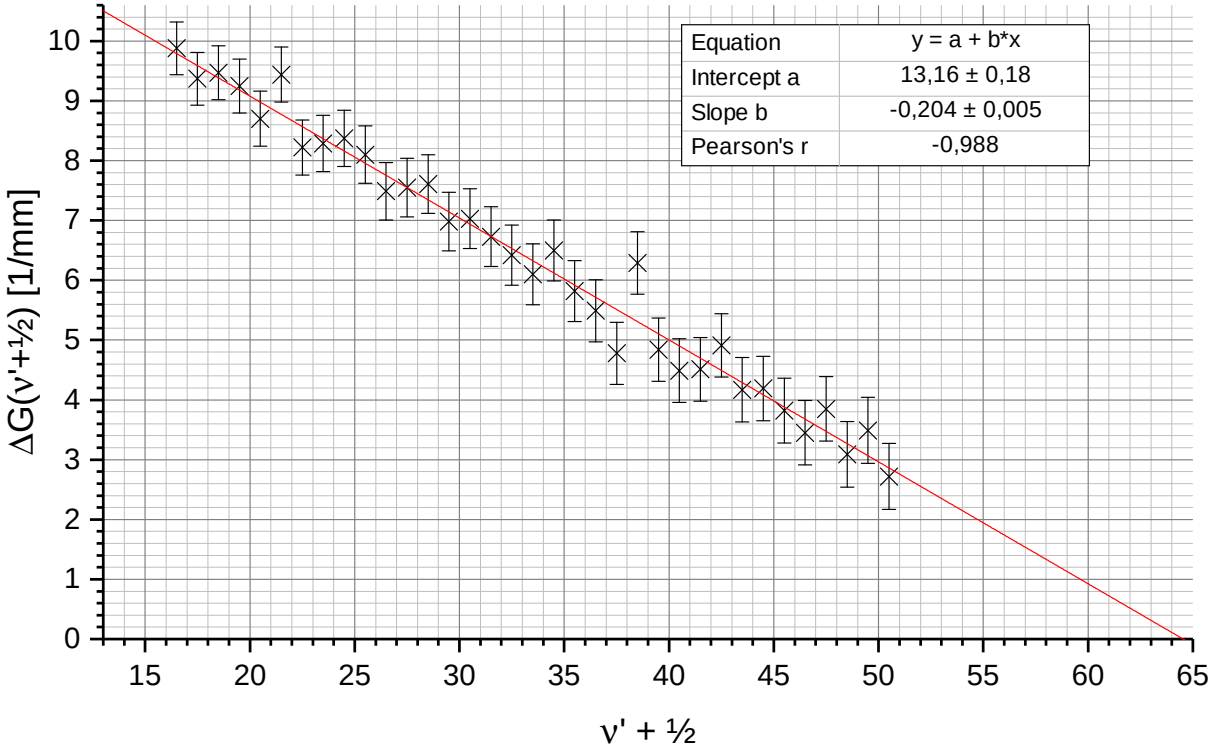

Figure 8: Birge-Sponer plot for $\nu'' = 0$ [1]

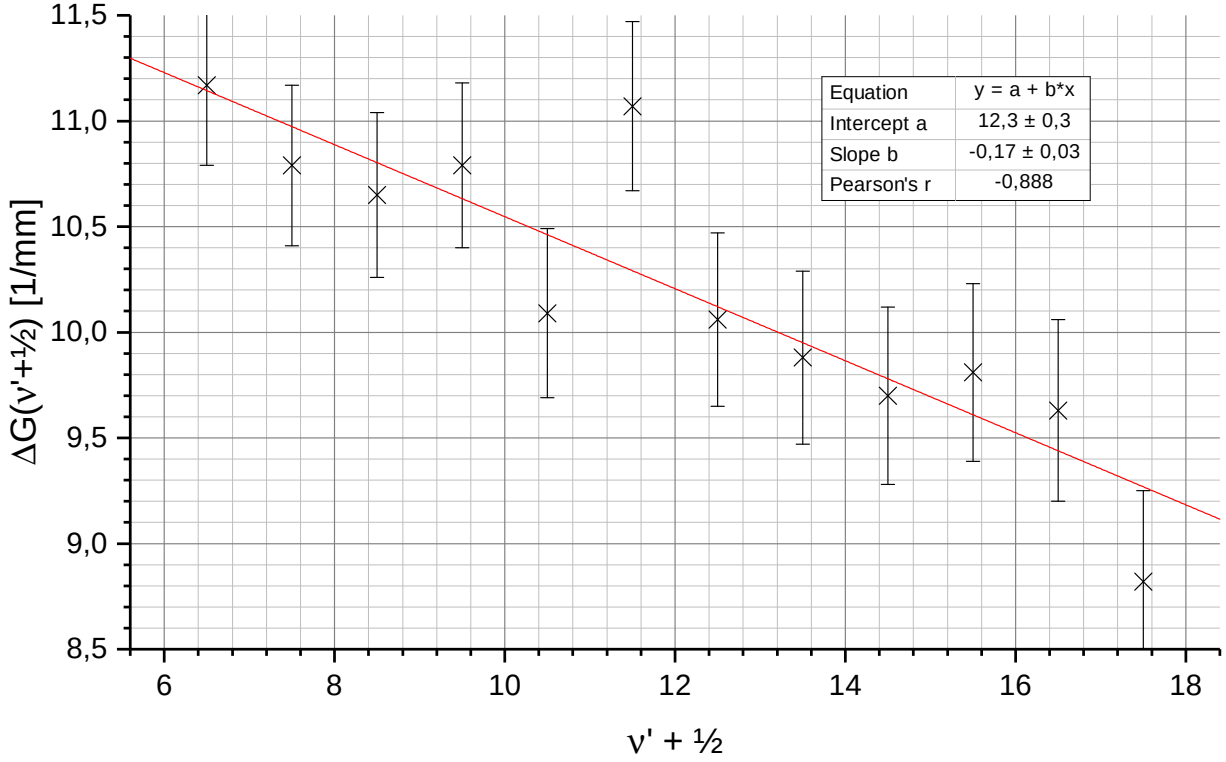

Figure 9: Birge-Sponer plot for $\nu'' = 1$ [1]

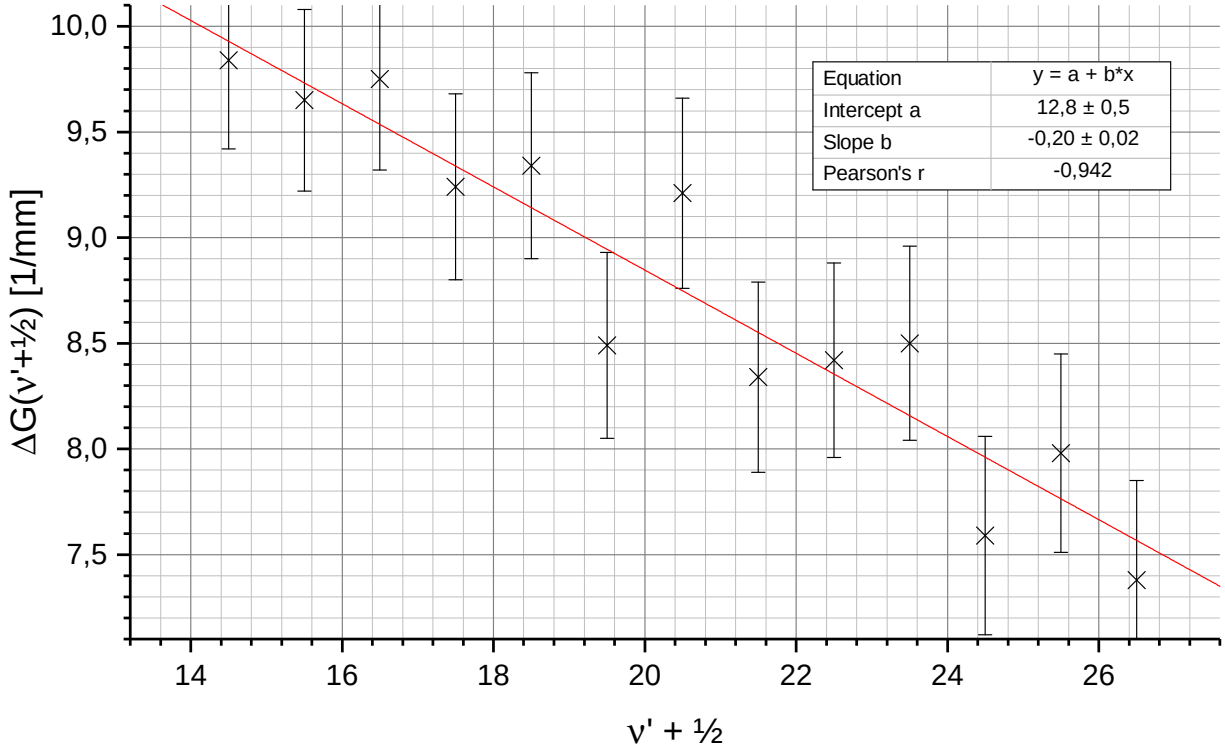

Figure 10: Birge-Sponer plot for $\nu'' = 2$ [1]

As you can see we did a linear fit $y = a + b \cdot x$. The intercept with the y-axis a and the slope b can be read out of the diagrams and can also be seen in Table 5.

ν''	Intercept a $[\frac{1}{\text{mm}}]$	Slope b $[\frac{1}{\text{mm}}]$
0	$13{,}16 \pm 0{,}18$	$-0{,}204 \pm 0{,}005$
1	$12{,}3 \pm 0{,}3$	$-0{,}17 \pm 0{,}03$
2	$12{,}8 \pm 0{,}5$	$-0{,}20 \pm 0{,}02$

Table 5: Slope and intercept of the different linear regressions

Because we want to calculate the oscillation constants x_e and $\omega_e x_e$ we have to change the linear equation. We have the formula 9

$$\begin{aligned}\Delta G(\nu' + \frac{1}{2}) &= \omega_e - \omega_e x_e (2\nu' + 2) \qquad \text{with} \quad \nu' + \frac{1}{2} = x \Leftrightarrow \nu' = x - \frac{1}{2} \\ &= \omega_e - \omega_e x_e ((2x - 1) + 2) \\ &= \underbrace{\omega_e - \omega_e x_e}_{\text{intersection } a} \underbrace{-2\omega_e x_e}_{\text{slope } b} x\end{aligned}$$

and so we can compute the oscillation constants

$$\begin{aligned}\omega_e x_e &= -\frac{b}{2} \\ s_{\omega_e x_e} &= \frac{s_e}{2} \\ \omega_e &= a + \omega_e x_e \\ s_{\omega_e} &= \sqrt{s_a^2 + s_{\omega_e x_e}^2}.\end{aligned}$$

We obtain the following values shown in Table 6.

ν''	$\omega_e x_e$ $[\frac{1}{mm}]$	ω_e $[\frac{1}{mm}]$
0	$0{,}102 \pm 0{,}003$	$13{,}26 \pm 0{,}18$
1	$0{,}085 \pm 0{,}014$	$12{,}3 \pm 0{,}3$
2	$0{,}099 \pm 0{,}012$	$12{,}9 \pm 0{,}5$

Table 6: Calculated oscillation constants $\omega_e x_e$ and ω_e

The constants should be equal. To combine all three values we compute the weighted mean

$$\begin{aligned} \bar{x} &= \frac{\sum_{i=1}^{n} (x_i / s_i^2)}{\sum_{i=1}^{n} (1/s_i^2)}, \\ s_{\bar{x}} &= \frac{1}{\sqrt{\sum_{i=1}^{n} (1/s_i^2)}}. \end{aligned} \tag{15}$$

So we get

$$\begin{aligned} \overline{\omega_e x_e} &= (0{,}101 \pm 0{,}003)\, \frac{1}{\text{mm}} \qquad \text{and} \\ \overline{\omega_e} &= (13{,}04 \pm 0{,}15)\, \frac{1}{\text{mm}}. \end{aligned}$$

5.3 Dissociation energy D_e

5.3.1 Dissociation energy D_e with the Birge-Sponer plot

For calculating the dissociation energy with help of the Birge-Sponer plot we need the intersection with the x-axis. Again we use the weighted mean (see formula 15) to combine all slopes and all intersections with the y-axis of the three linear equations. We obtain the values

$$\begin{aligned} \bar{a} &= (12{,}94 \pm 0{,}15)\, \frac{1}{\text{mm}}, \\ \bar{b} &= (-0{,}203 \pm 0{,}005)\, \frac{1}{\text{mm}}. \end{aligned}$$

Now we can compute the intersection with the x-axis by

$$\begin{aligned} & \Delta G(\nu_{\text{diss}} + \frac{1}{2}) = 0 \\ \Leftrightarrow & \bar{a} + \bar{b}(\nu' + \frac{1}{2}) = 0 \\ \Leftrightarrow & \nu_{\text{diss}} = -\frac{\bar{a}}{\bar{b}} - \frac{1}{2} \\ & s_{\nu_{\text{diss}}} = \sqrt{\left(\frac{s_{\bar{a}}}{\bar{b}}\right)^2 + \left(\frac{\bar{a}}{\bar{b}} s_{\text{diss}}\right)^2}, \end{aligned}$$

and so we get

$$\nu_{\text{diss}} = 63{,}4 \pm 1{,}8.$$

With formula 10 we can compute the dissociation energy

$$\begin{aligned} D_0 &= \sum_{\nu=0}^{\nu_{\text{diss}}} \Delta G\left(\nu+\frac{1}{2}\right) = \sum_{\nu=0}^{\nu_{\text{diss}}} a+b\cdot\left(\nu+\frac{1}{2}\right) \\ &= (\nu_{\text{diss}}+1)\cdot a+(\nu_{\text{diss}}+1)\cdot\frac{b}{2}+b\cdot\sum_{\nu=0}^{\nu_{\text{diss}}} j \\ &= (\nu_{\text{diss}}+1)\cdot\left(a+\frac{b}{2}\right)+b\cdot\frac{\nu_{\text{diss}}\cdot(\nu_{\text{diss}}+1)}{2} \\ &= a\cdot\nu_{\text{diss}}+b\cdot\nu_{\text{diss}}+\frac{b}{2}\cdot\nu_{\text{diss}}^2+a+\frac{b}{2} \end{aligned} \tag{16}$$

with the uncertainty

$$s_{\text{D}_0} = \sqrt{((a+b+b\cdot\nu_{\text{diss}})\cdot s_{\nu_{\text{diss}}})^2+((\nu_{\text{diss}}+1)\cdot s_{\text{a}})^2+\left(\left(\nu_{\text{diss}}+\frac{\nu_{\text{diss}}^2}{2}+\frac{1}{2}\right)\cdot s_{\text{b}}\right)^2}, \tag{17}$$

and so we obtain

$$D_0 = (414\pm 15)\,\frac{1}{\text{mm}}.$$

Next step is to calculate $G(0)$ with formula 8

$$\begin{aligned} G(0) &= \frac{1}{2}\omega_{\text{e}}-\frac{1}{4}\omega_{\text{e}}x_{\text{e}}, \\ s_{\text{G}_0} &= \sqrt{\left(\frac{s_{\omega_{\text{e}}}}{2}\right)^2+\left(\frac{s_{\omega_{\text{e}}\text{x}_{\text{e}}}}{4}\right)^2}. \end{aligned}$$

The value is

$$G(0) = (6{,}50\pm 0{,}08)\,\frac{1}{\text{mm}}.$$

Now we can easily determine the dissociation energy D_{e} by

$$\begin{aligned} D_{\text{e}} &= D_0+G(0), \\ s_{\text{D}_{\text{e}}} &= \sqrt{(s_{\text{D}_0})^2+(s_{\text{G}(0)})^2}. \end{aligned}$$

The given values above results to a dissociation energy

$$D_{\text{e}} = (420\pm 15)\,\frac{1}{\text{mm}}.$$

5.3.2 Dissociation energy D_{e} with the Morse potential

It is also possible to calculate the dissociation energy D_{e} with the Morse potential. With formula 12 we get

$$\begin{aligned} D_{\text{e}} &= \frac{\omega_{\text{e}}^2}{4\omega_{\text{e}}x_{\text{e}}}, \\ s_{\text{D}_{\text{e}}} &= D_{\text{e}}\cdot\sqrt{\left(2\cdot\frac{s_{\omega_{\text{e}}}}{\omega_{\text{e}}}\right)^2+\left(\frac{s_{\omega_{\text{e}}\text{x}_{\text{e}}}}{\omega_{\text{e}}x_{\text{e}}}\right)^2}. \end{aligned} \tag{18}$$

The result is of the dissociation energy is

$$D_{\text{e}} = (420\pm 16)\,\frac{1}{\text{mm}}.$$

5.4 Dissociation energy E_{diss}

To determine the dissociation energy E_{diss} we have to look at the absorption spectrum. The area we are now interested in is the lowest wavelength where absorption is possible. That means the highest energy a iodine electron can absorb before it leaves the molecule.

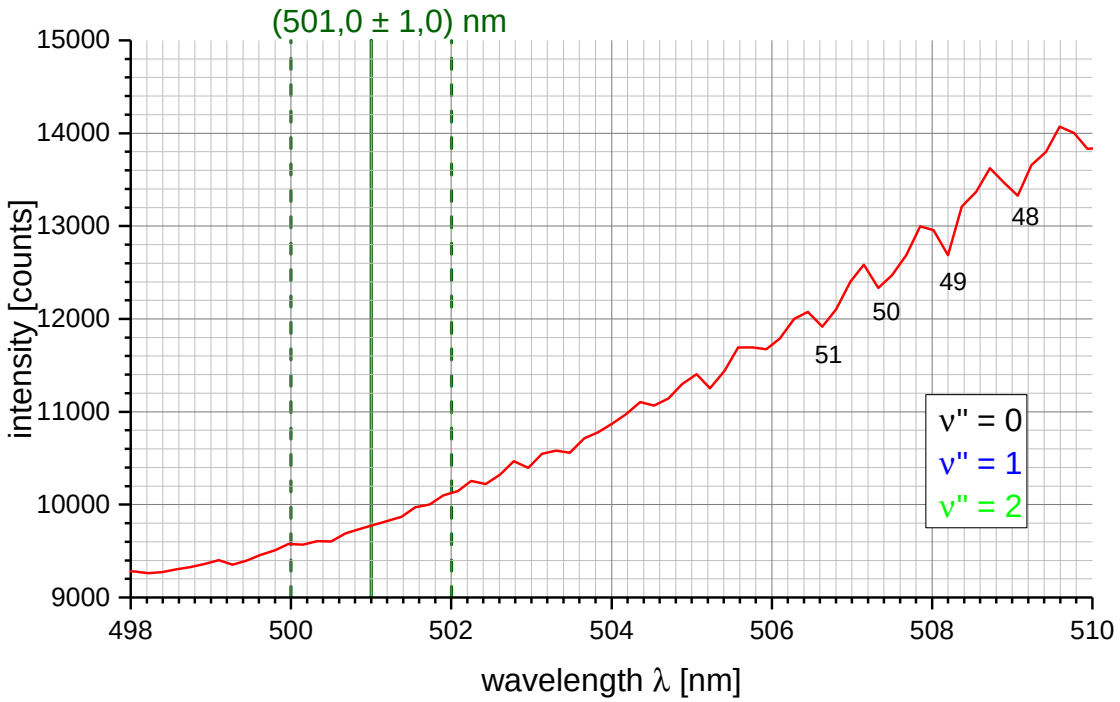

Figure 11: Lowest wavelength area of the absorption spectrum where absorption can be detected [1]

From Figure 11 we read out a wavelength $\lambda_{\mathrm{min}} = (501{,}0 \pm 1{,}0)\,\mathrm{nm}$. With the systematic displacement $\lambda_{\mathrm{displacement}} = (0{,}4 \pm 0{,}1)\,\mathrm{nm}$ (see chapter 5.1), which has a comparatively small and negligible error, and

$$E_{\mathrm{diss}} = \frac{1}{\lambda_{\mathrm{min}} + \lambda_{\mathrm{displacement}}}$$
$$s_{\mathrm{E_{diss}}} = \frac{s_{\lambda_{\mathrm{min}}}}{(\lambda_{\mathrm{min}} + \lambda_{\mathrm{displacement}})^2}$$

it follows

$$E_{\mathrm{diss}} = (1994 \pm 4)\,\frac{1}{\mathrm{mm}}.$$

5.5 Excitation energy T_{e}

The excitation energy T_{e} is the energy difference between the lowermost states of the ground and the excited state. So it is calculable with

$$T_{\mathrm{e}} = E_{\mathrm{diss}} - D_0,$$
$$s_{\mathrm{T_e}} = \sqrt{(s_{\mathrm{diss}})^2 + (s_{\mathrm{D_0}})^2}$$

and the result is

$$T_{\mathrm{e}} = (1580 \pm 16)\,\frac{1}{\mathrm{mm}}.$$

5.6 Morse potential of the excited state

The aim of this part is to draw the Morse potential of the excited state

$$E_{\mathrm{pot}}(R) = D_{\mathrm{e}} \cdot \left[1 - e^{-a(R-R_{\mathrm{e}})}\right]^2.$$

D_{e} is already known from a previous part (section 5.3.1). With formula 5 we can calculate the constant

$$a = \sqrt{\frac{4\pi c\mu \cdot \omega_{\mathrm{e}} x_{\mathrm{e}}}{\hbar}} = 194{,}9\,\text{Å}. \tag{19}$$

For the energetic favourable state $R_{\mathrm{e}} = 2{,}979\,\text{Å}$ [5](page 11) we use a literature value. The computed Morse potential is drawn in Figure 12.

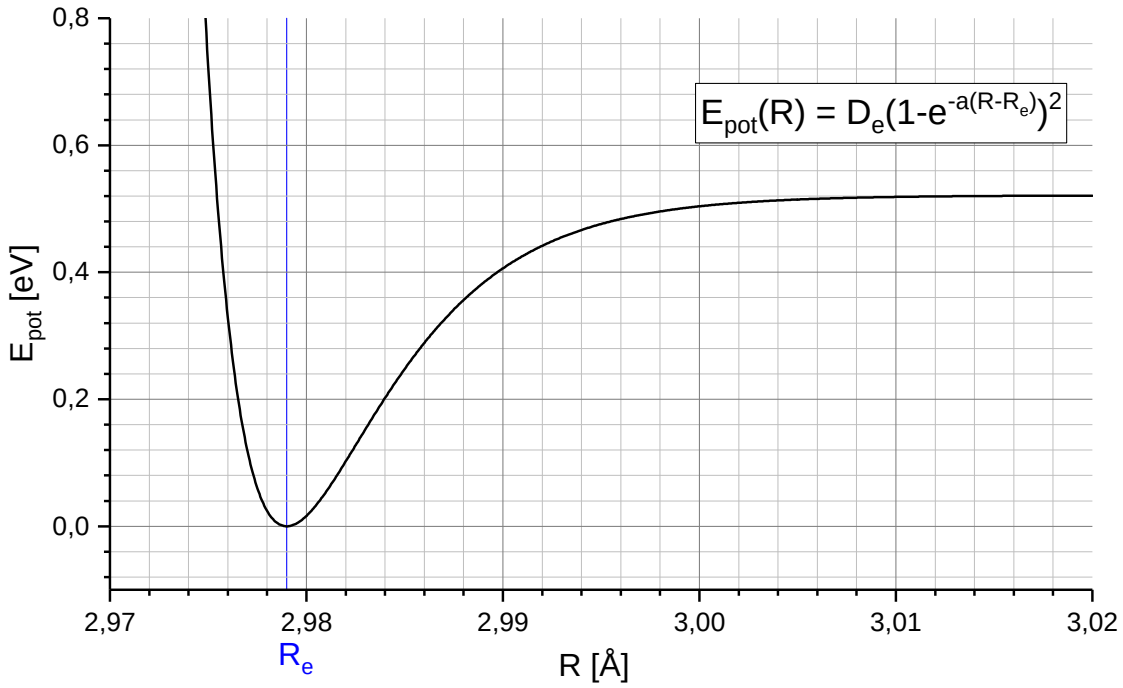

Figure 12: Morse potential of the excited state [1]

5.7 Emission spectrum

At first we have done a measurement for calibrating the monochromator with the help of a mercury lamp. The characteristic spectrum is shown in Figure 13.

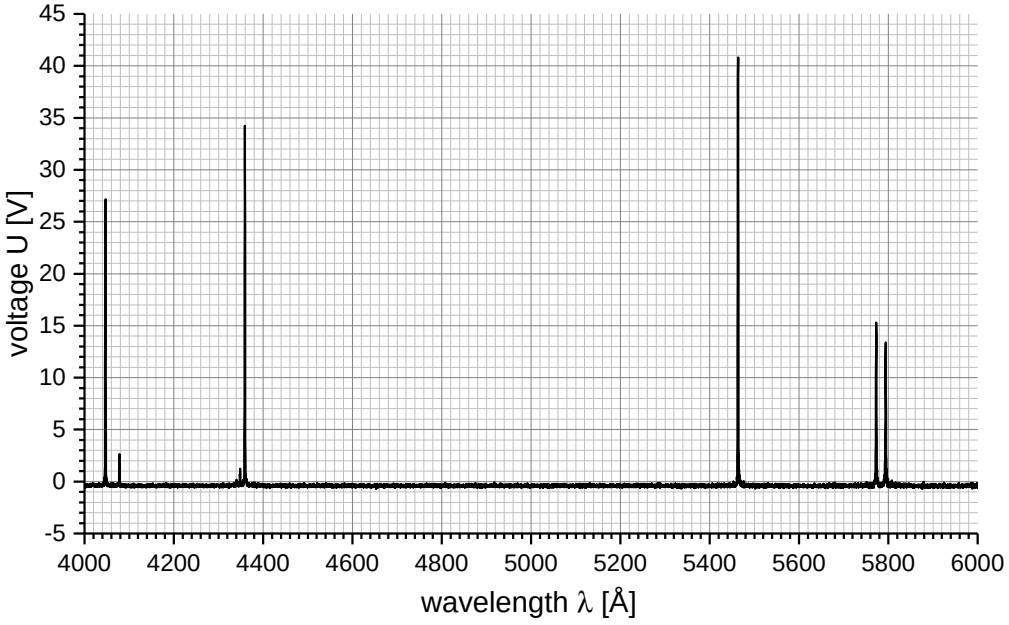

Figure 13: Emission spectrum of the mercury lamp [1]

After that we measured the spectrum of the area around the wavelength of the laser. The resonance peak is shown in Figure 14.

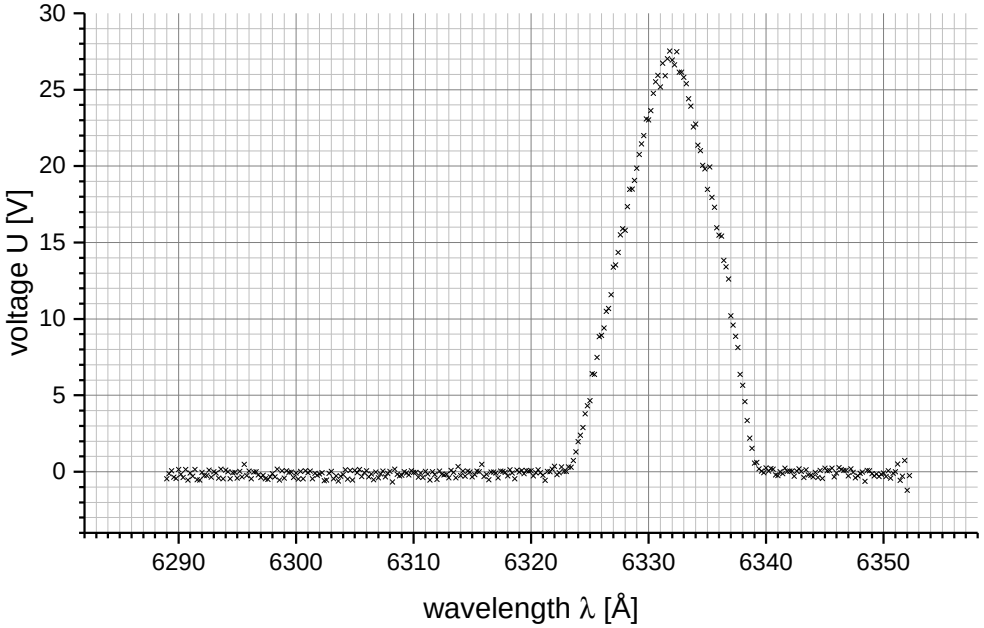

Figure 14: Resonance peak of the helium-neon laser [1]

The last step was to measure the whole emission spectrum of iodine. Here we had problems with the measurement which are discussed in the discussion (cf. section 6.2). They made it impossible to continue the measurement. We tried to measure the maximum of the iodine

spectrum at ca. $6495 - 6510\,\text{Å}$. Therefore we computed a average of ten measurements and plot the data which are shown in Figure 15 and we plot the best single measurement which is shown in Figure 16.

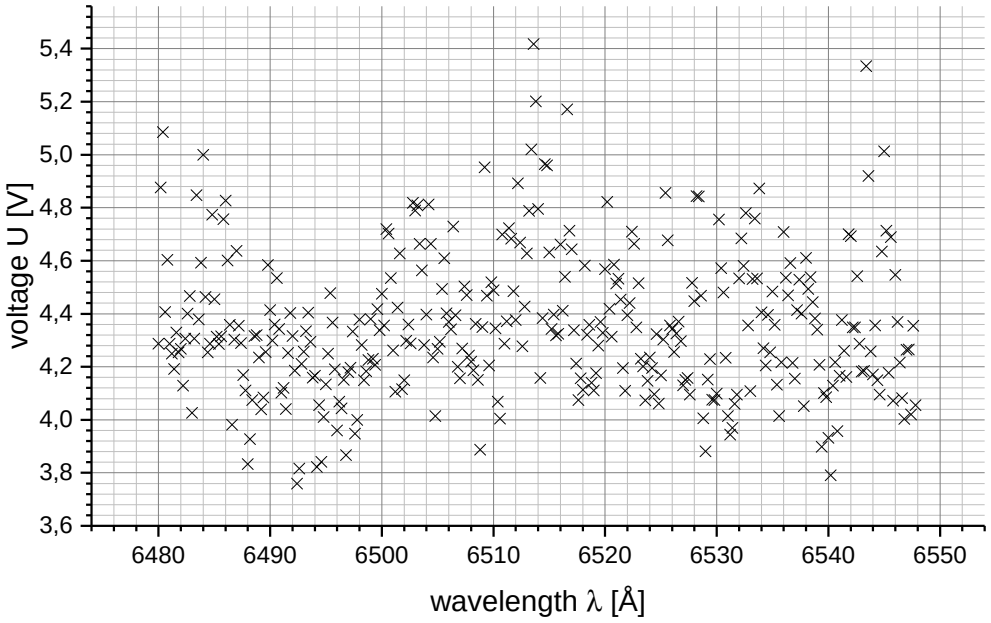

Figure 15: Average of 10 measurements of the maximum of the iodine emission spectrum [1]

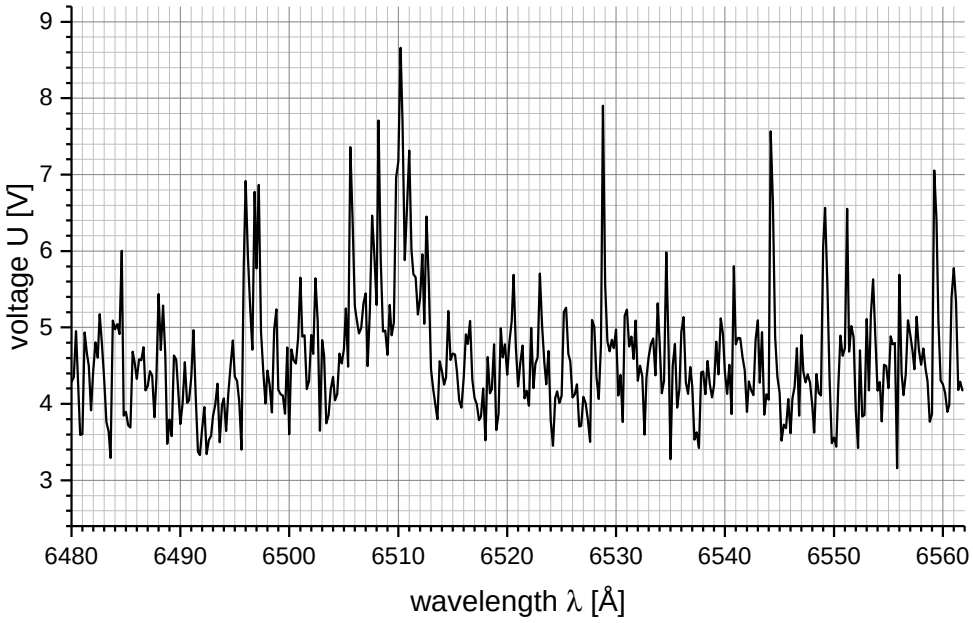

Figure 16: Measurement of the maximum of the iodine emission spectrum [1]

6 Discussion

6.1 Absorption

The aim of this experiment part was to get the parameters ω_e and $\omega_e x_e$, the dissociation energies D_0, D_e and E_{diss} and the excitation energy T_e. To reduce the statistic errors we measured 10.000 times and take the mean. More measurements wouldn't give a helpful improved signal. By the numbering of the peaks of the progression $\nu'' = 0$ we supposed no error, because the start value is a literature value. The numbering of the other progressions via comparison of distances is probably correct, but still a potential source of error. With a look on the Birge-Sponer plots of the different progressions one can see that the assumption of a linear correlation between ν' and $G(\nu')$ is justified. A confirmation for it are the Pearson's r coefficients of the linear regressions which are all lower $-0,88$. But it is also visible that nearly all error bars have a intersection with the linear regression. Therefore the error of the readout wavelengths $s_\lambda = 0{,}1\,\text{nm}$ was maybe a bit to small estimated.

To check the quality of our measurements and the resultant values we compare them with literature values in Table 7.

	measured value $[\frac{1}{\text{cm}}]$	literature value $[\frac{1}{\text{cm}}]$	variation
ω_e	$130{,}4 \pm 1{,}5$	$125{,}69$[6]	4σ
$\omega_e x_e$	$1{,}01 \pm 0{,}03$	$0{,}764$[6]	9σ
D_e (Birge-Sponer)	4200 ± 150	4391[7]	2σ
D_e (Morse potential)	4200 ± 160	4391[7]	2σ
E_{diss}	$19\,940 \pm 40$	$20\,014$[7]	2σ
T_e	$15\,800 \pm 160$	$15\,769$[6]	1σ

Table 7: Comparison with literature values

The values ω_e and $\omega_e x_e$ are weighted means of the three progression, so the values of progression $\nu'' = 0$ are more important than the others because of the many measuring points. But these are also the worst values, so the results are far away form the literature values. In addition the $\omega_e x_e$-values are for all three progressions too high, so we suppose a systematic error. A statistical error can be, based on the many measuring points, eliminated. Contemplable is also a mistake from us, but we can't remember something, which can be origin of this.
Both calculation methods for D_e produce the same result, just the related errors differ a little bit. Possibly the calculations are very similar. The value has a 2σ-variation to the literature value, this is a acceptable result. This also applies for the dissociation energy E_{diss}. The reason for the uncertainty is the very difficult read-out of the disappearance of the peaks. The excitation energy T_e fits very well to the literature value. Because it is a difference of two calculated values it is also possible that the errors reduce each other.
At the start of the analysis we mentioned the displacement of the wavelength of $(0{,}4 \pm 0{,}1)\,\text{nm}$. It is also possible that the justification of the spectrometer has a greater error than supposed and the displacement of the wavelength is more than one peak. To eliminate such an error a calibration with a known material would have been helpful. Such a displacement could explain the 9σ-variation of $\omega_e x_e$.
To improve the experiment further a better spectrometer with a higher resolution would be helpful. This would allow to specify the peaks and minimise the uncertainties.

6.2 Emission

As we said in the analysis the measurement of the emission spectrum of iodine failed. Here we want to describe in a short way what we have done to try to get a better signal and possible reasons why it went wrong.
First step was to heat up the iodine tube with 2 blowers to get more gaseous iodine molecules. We tried to keep the tube as hot as possible during the whole implementation. After that we tried to shade the setup with a black cloth and black little movable walls. We also switch out the lights and turn off the PC display during a measurement. The discriminator settings were adjusted to the expected voltage amplitude. With this improvements of the setup we tried to get the maximum of iodine spectrum. We had to assert that there is no signal at all. So we decided to change the split width because maybe the lens focus the light next to it. However this does not change the signal, too. After that we change the position of the lens and again tried to get a better signal. It failed. We thought that there is a little peak at the desired place, so we measured ten times and calculate the mean of all values but this did not work, too. In view of the fact that we tried a lot of tricks to get any useful values and still failed we decided to stop the measurement.
Maybe there were not enough gaseous iodine molecules and as a consequence there were not enough photons for separating them from the noise. Another reason that explains a missing signal is a wrong setting of the focus of the lens. Maybe the light did not strike to the split and so the monochromator is not able to measure a signal. However we think that this is unlikely because we checked it by holding a torch behind the iodine tube and set the focus in a right way. It is to mention that the way of the laser beam through the iodine is very short. To measure a (stronger) signal a extension of the way through the iodine, for example by reflection, could help.

7 Attachment

7.1 Spectrometer

In the experiment we used a spectrometer. Because it is not necessary for the implementation to know how it works but it is a great component of the setup we will describe its functionality here. You can see one in Figure 17.

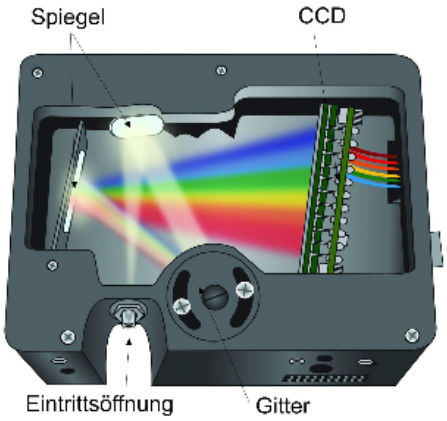

Figure 17: Sketch of the used spectrometer [3]

To measure a light you have to focus it to the opening of the spectrometer. Inside the light strikes to a mirror and then to a lattice. Here the light will be diffract. With having another mirror and so a longer way to the detector brighter split up can be achieved. Because of this brighter split up it is easier for a CCD chip to registers a different between different wavelengths. The CCD chips gives the information about the diffraction pattern to a PC.

7.2 Monochromator

For the second part of the experiment we used a monochromator. A schematic sketch is shown in Figure 18

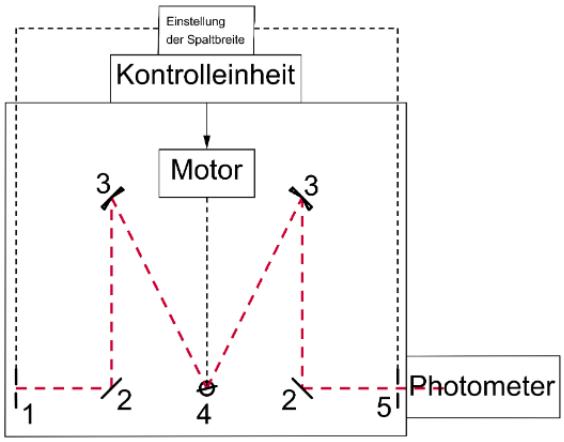

Figure 18: Sketch of the used monochromator [3]

The monochromator consists of an entrance for the light, a slit with variable width. After the slit there is a plane mirror and a curved mirror which transfer the light to a lattice. It

separates the light into the spectrum and transfer it to two other mirrors to the exit slit. Behind the slit is a photometer which measured the intensity. The lattice is rotatable so a huge spectrum is measurable. The rotating velocity and split width can be adjusted at the control unit.

7.3 Plots

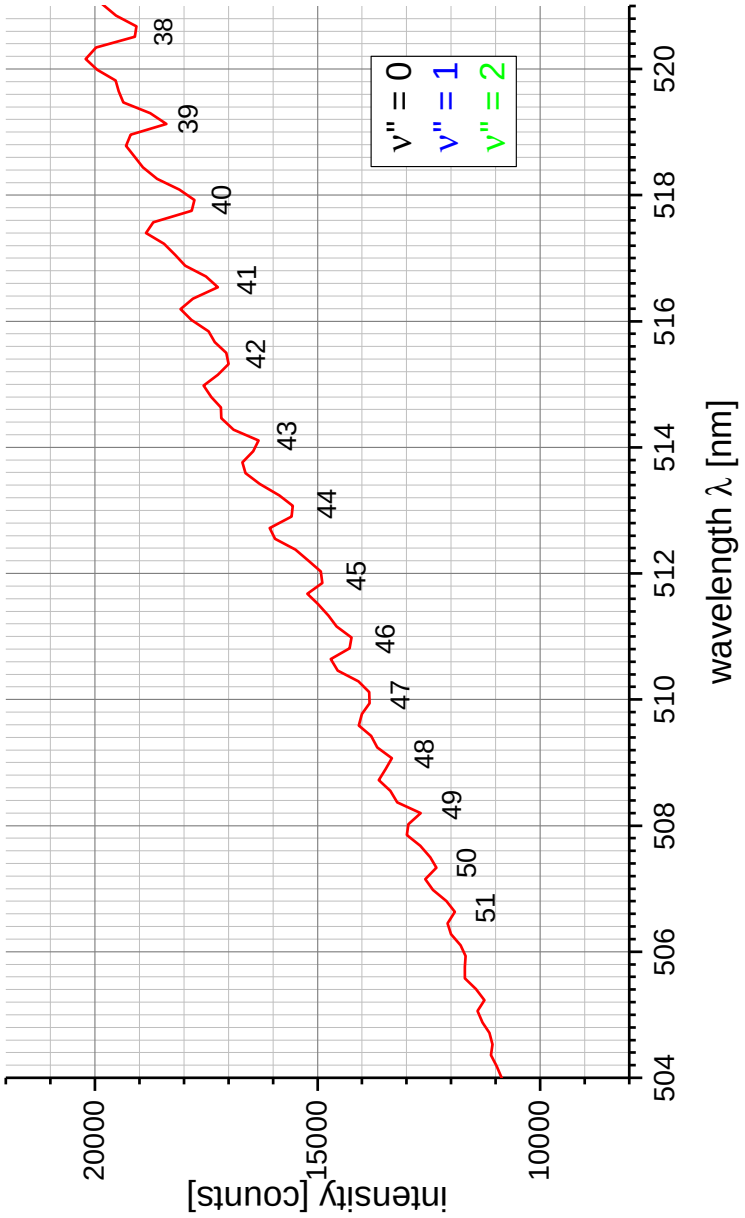

Figure 19: Absorption spectrum ($500-520\,\mathrm{nm}$) with numbered transitions [1]

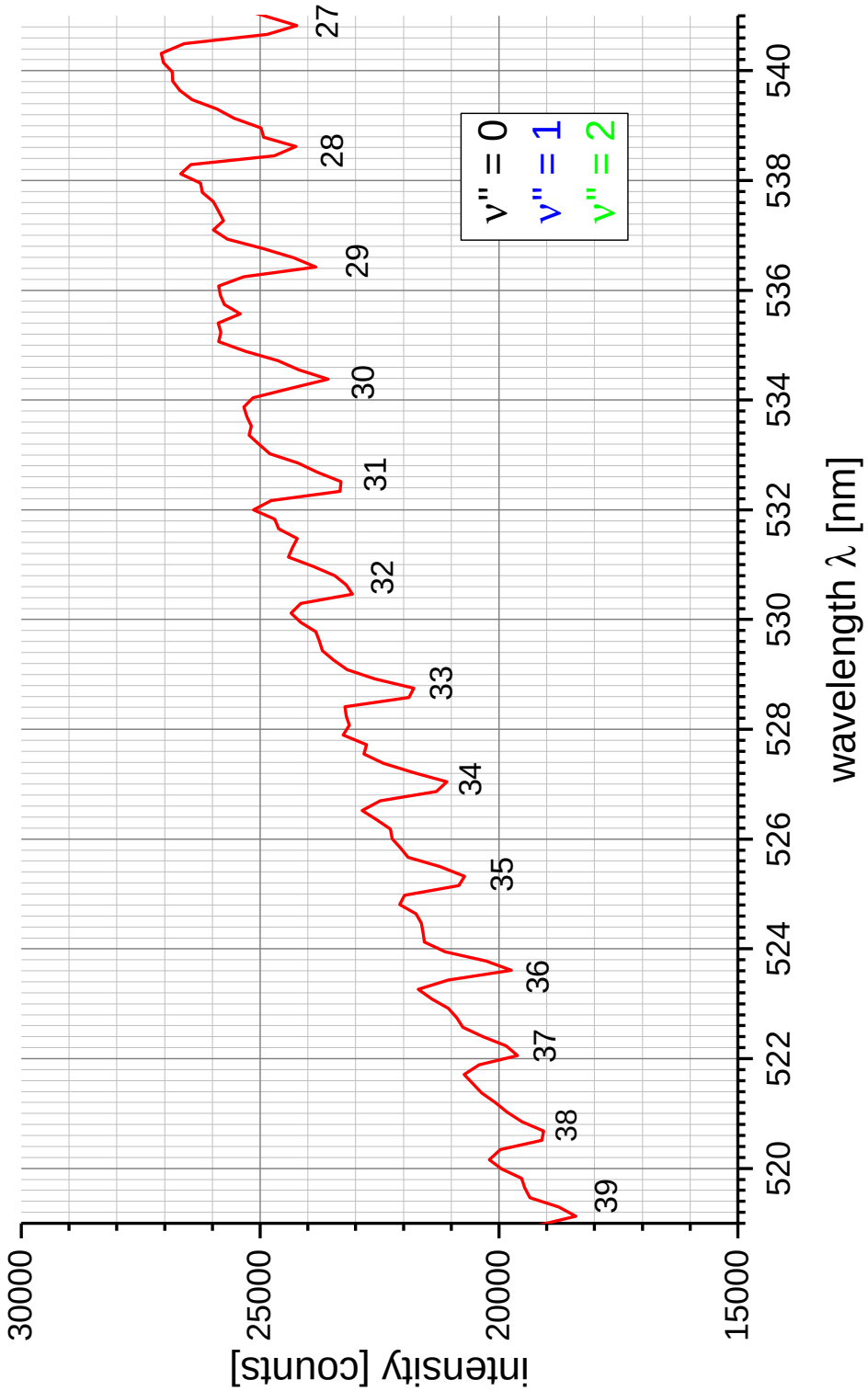

Figure 20: Absorption spectrum ($520 - 540\,\mathrm{nm}$) with numbered transitions [1]

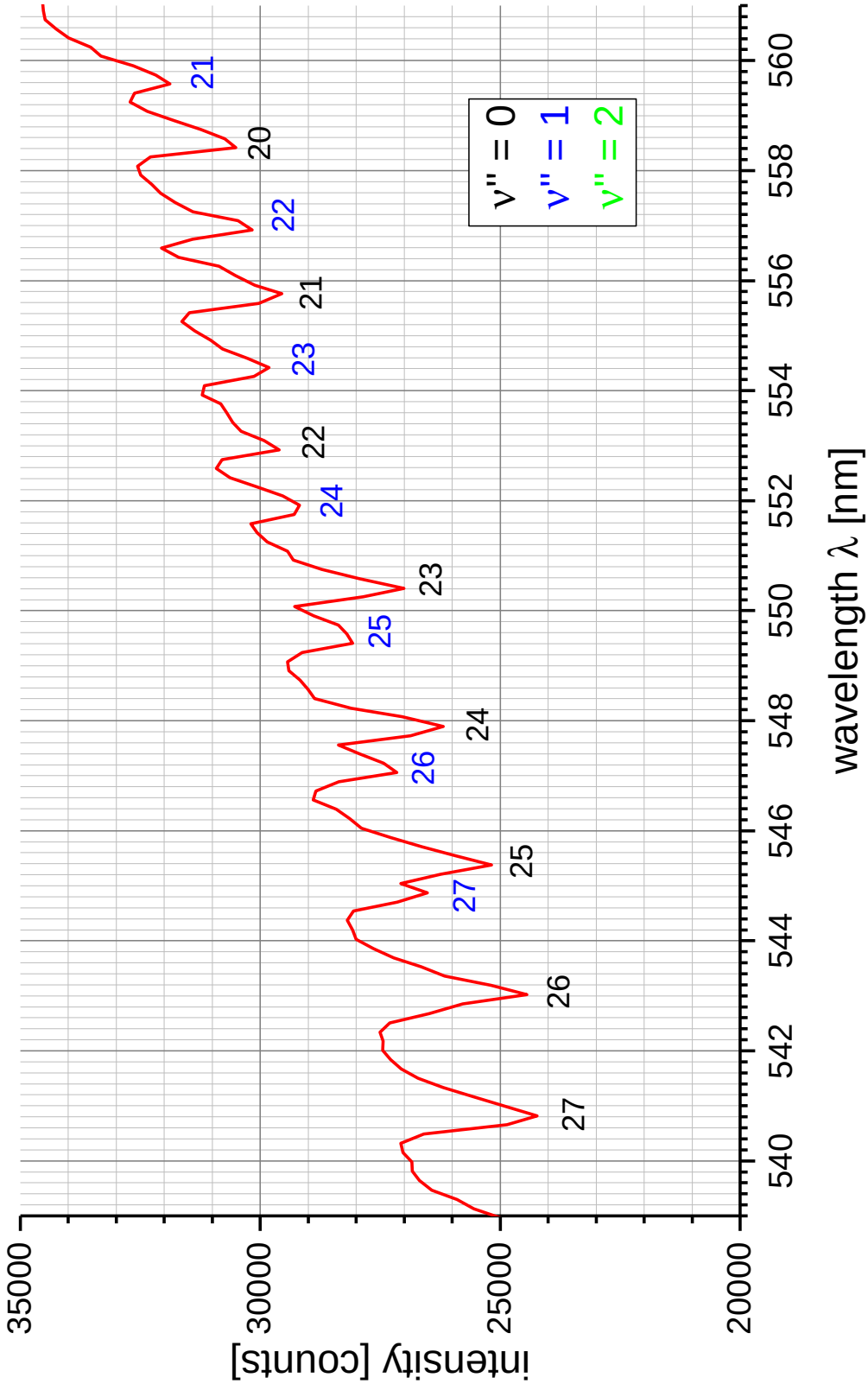

Figure 21: Absorption spectrum ($540-560\,\mathrm{nm}$) with numbered transitions[1]

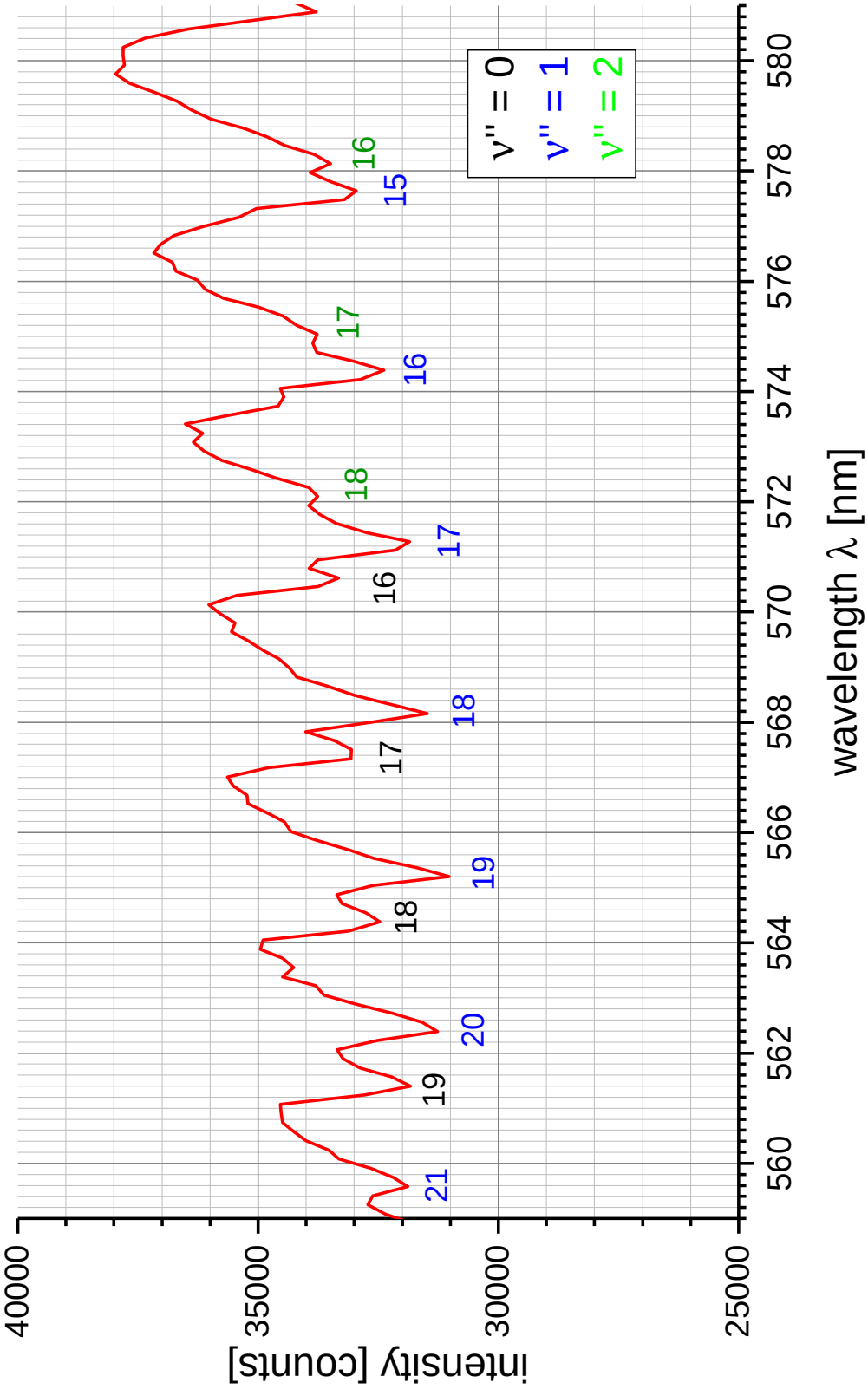

Figure 22: Absorption spectrum ($560 - 580\,\mathrm{nm}$) with numbered transitions [1]

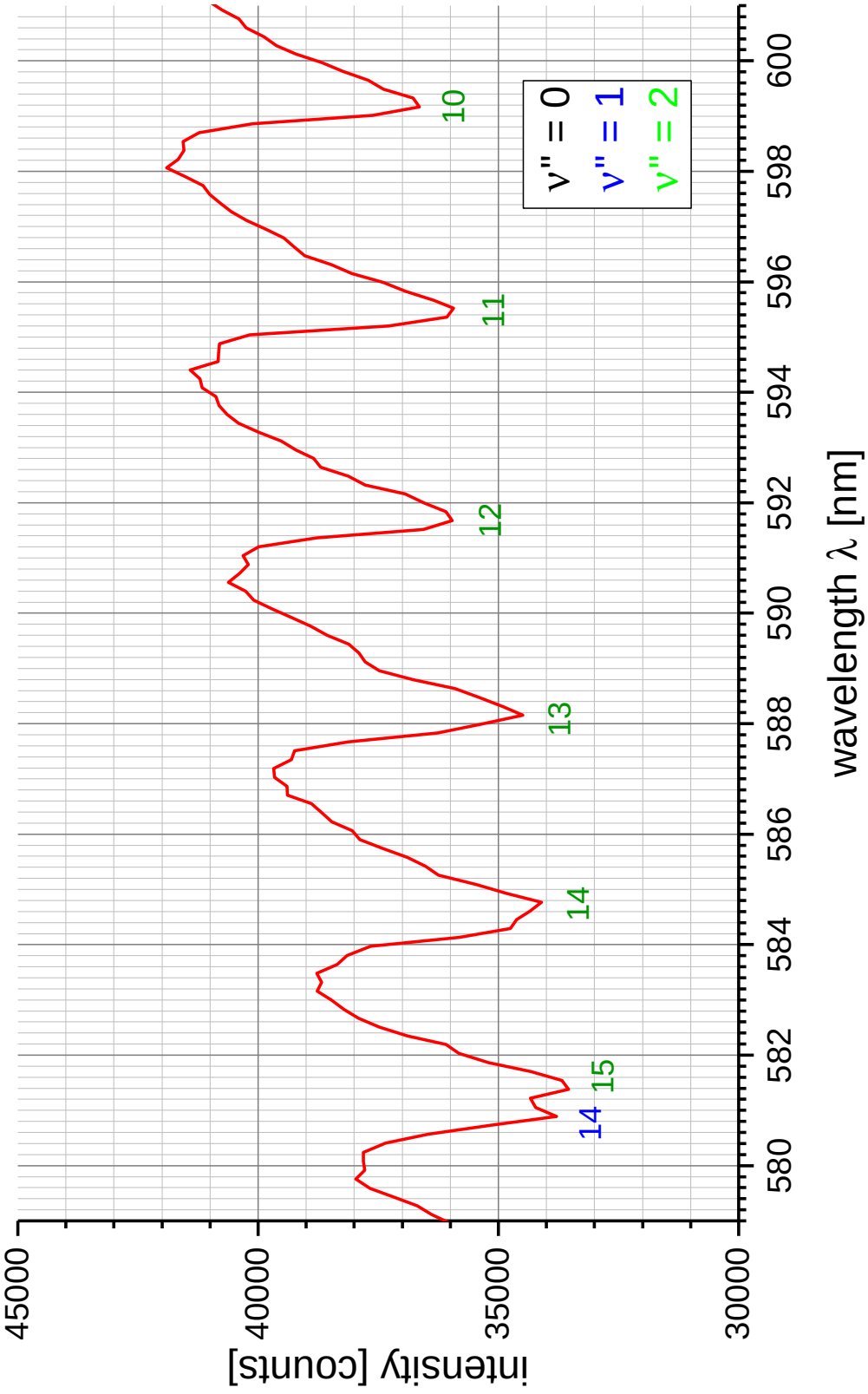

Figure 23: Absorption spectrum ($580 - 600\,\mathrm{nm}$) with numbered transitions [1]

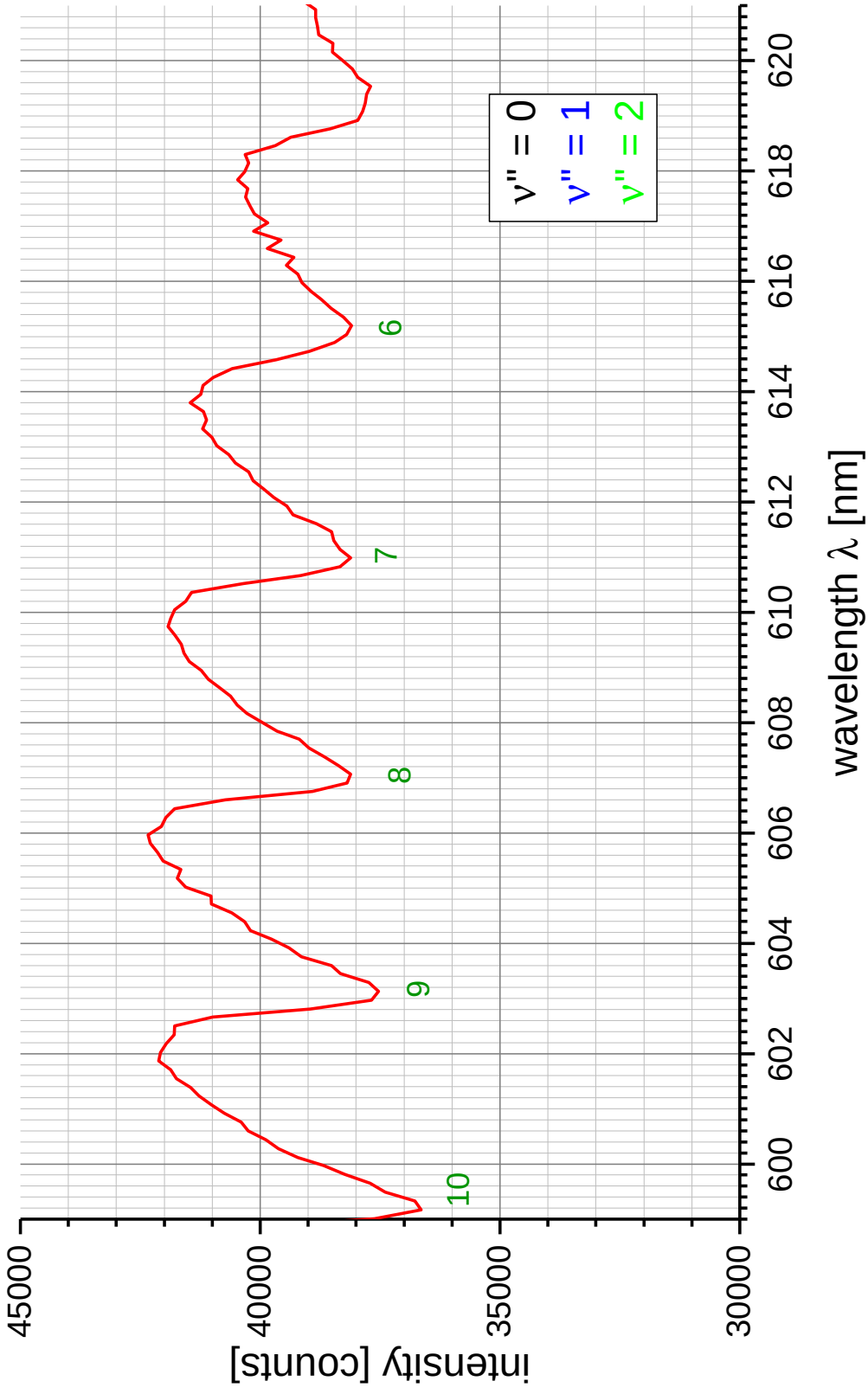

Figure 24: Absorption spectrum ($600 - 620\,\mathrm{nm}$) with numbered transitions [1]

References

[1] The diagram was generated with OriginPro 2017G.

[2] Self-made with Open Office

[3] Versuchsanleitung Fortgeschrittenenpraktikum Teil 1 - Spektroskopie am Jod-Molekül [http://hacol13.physik.uni-freiburg.de/fp/Versuche/FP1/FP1-16-J2-Molekuel/Anleitung_SA.pdf] (called on 13.09.2017)

[4] Klaus Bitsch- Aufbau einer Apparatur fürs Fortgeschrittenen-Praktikum: "Untersuchung der Schwingungsstruktur des $X^1\Sigma^+_{0g} \leftrightarrow B^3\Pi^+_{0u}$-Übergangs beim I_2-Molekül" (1977) [http://hacol13.physik.uni-freiburg.de/fp/Versuche/FP1/FP1-16-J2-Molekuel/Staatsex-Jod2-Molekuel.pdf] (called on 13.09.2017)

[5] Martine Meyer-Verbesserung des Versuchs Spektroskopie am J_2-Molekül des Fortgeschrittenen-Praktikums (2014) [http://hacol13.physik.uni-freiburg.de/fp/Versuche/FP1/FP1-16-J2-Molekuel/Staatsexamensarbeit.pdf] (called on 13.09.17)

[6] [http://webbook.nist.gov/cgi/cbook.cgi?ID=C7553562&Mask=1000] (called on 17.09.2017)

[7] Steinfeld, J. et al: Spectroscopic Constants and Vibrational Assignment for the B 3 + ou State of Jodine , Journal of Chemical Physics 42 (1965) p. 25-33